Paper n. 056

A MULTIBLADE AERODYNAMIC REDUCED-ORDER MODEL FOR AEROELASTIC ANALYSIS OF HELICOPTER ROTORS IN FORWARD FLIGHT

M. Gennaretti and D. Muro

University Roma Tre
Dept. of Mechanical and Industrial Engineering
Via della Vasca Navale 79 - 00146 Rome, Italy
e-mail: m.gennaretti@uniroma3.it

Abstract

This paper presents a methodology for the identification of a Reduced-Order Model (ROM) describing the linearized unsteady aerodynamics of helicopter rotors in forward flight. It is defined in the multiblade coordinate nonrotating frame and yields a linear differential form relating the rotor blade motion to the corresponding aerodynamic loads. This approach requires the prediction of harmonic responses by an aerodynamic solver. The accuracy of the identified ROM in describing unsteady aerodynamics phenomena is strictly connected to that of the aerodynamic solver. Complex aerodynamic effects (like wake roll up, wake-blade interactions) are included in the ROM if they are taken into account in evaluating the harmonic responses. Preliminary numerical results concerning a flap-lag helicopter rotor in forward flight are presented, showing the calculated and approximated multiblade transfer functions from which the differential form of the ROM is obtained, along with the corresponding stability analysis compared with that from a static inflow aerodynamic model. An aeroservoelastic application is included in order to demonstrate the feasibility of the ROM proposed for control-law synthesis.

List of Symbols

$\mathbf{A}$	=multiblade state space constant matrix
$\mathbf{A}_i, \mathbf{G}, \mathbf{H}, \mathbf{R}$	=matrices of the rational approximation
$\mathbf{E}$	=transfer function matrix
$\mathbf{f}^B$	=vector of the aerodynamic forces in the rotating frame
$\mathbf{f}^M$	=vector of the aerodynamic forces in multiblade nonrotating frame
G	=unit source solution
$\mathbf{M}, \mathbf{C}, \mathbf{K}$	=mass, damping and stiffness matrices in the rotating frame
$\bar{\mathbf{M}}, \bar{\mathbf{C}}, \bar{\mathbf{K}}$	=average mass, damping and stiffness matrices in multiblade frame
N	=number of blades
$\mathbf{r}$	=additional aerodynamic states
t	=time
q^m	=m-th blade degree of freedom in the rotating frame
$q_0, q_{N/2}$	=collective and differential multiblade coordinates
q_{nc}, q_{ns}	=cyclic multiblade coordinates
$\mathbf{T}$	=matrix of multiblade transformation
$\mathbf{x}$	=observer position
$\mathbf{x}^B$	=blade coordinates
$\mathbf{x}^M$	=multiblade coordinates
$\mathbf{y}$	=source position
$\mathbf{z}$	=aeroelastic state variables
φ	=velocity potential
ω	=angular frequency

Introduction

The aim of this work is the development of a Reduced-Order Model (ROM) for the description of perturbation unsteady aerodynamic loads arising on helicopter rotor blades in forward flight conditions. The introduction of reduced-order aerodynamics modeling allows the eigenanalysis of aeroelastic problems with the evaluation of dampings and frequencies, and hence is particularly convenient for those applications that need accurate prediction tools at low computational costs (like, *e.g.,* preliminary design). In addition, it may be applied to express the aeroelastic system in a form appropriate for control-law identification, and hence is particularly suited for aeroservoelastic purposes.

In the past, reduced-order models for rotor aerodynamics have been obtained by strip-theory approaches based on the Loewy and Greenberg theories, with approximated rational forms of the lift deficiency function (see, for instance, [1]). However, widely applied aerodynamic ROMs for rotorcraft configurations are those that have been developed by Peters and his co-workers (see for instance, [2], [3], [4]). They are based on the finite-state approximation of the wake inflow affecting the aerodynamic loads

arising on the rotor blades, and have inspired the work of many of the researchers interested in rotor aeroelasticity analysis. In these models the aerodynamic loads are not derived from first principles, but rather are obtained coupling blade sectional loads and wake vorticity effects and are strongly dependent on the wake shape. Several model of different complexity have been developed in the last years, taking into account wake distortion effects (see, for instance, [5] and [6]).

Here, we present an approach aimed at the identification of a linear aerodynamic ROM for the perturbation analysis of helicopter rotors in forward flight, defined in terms of multiblade coordinates in the nonrotating frame. It requires the availability of a time-marching aerodynamic solver for the evaluation of rotor harmonic responses and yields a constant-coefficient differential model relating multiblade rotor coordinates to the (generalized) aerodynamic forces in the nonrotating frame. As it will be explained later, it relies on the rational approximation of the matrix collecting the multiblade transfer functions determined through the harmonic responses, which is carried out by the approach described in [7]. From this point of view, this method is inspired to the fixed-wing, finite-state formulations investigated by Vepa [8], Edwards [9], Roger [10], and particularly to that applied by Karpel [11]. Note that the accuracy of the identified aerodynamic ROM depends on the accuracy of the aerodynamic solver applied for the harmonic responses and, if allowed by the solver capabilities, may take into account complex aerodynamic effects with inclusion of wake roll-up and blade-vortex interaction.

In the following, the ROM identification procedure will be explained in details; next, for a flap-lag rotor in forward flight, multiblade transfer functions derived from the aerodynamic solver and approximated ones will be illustrated and discussed, and corresponding preliminary results concerning the aeroelastic stability analysis will be presented.

ROM identification

When a finite-state aerodynamic model is applied for the simulation of the perturbed motion of helicopter rotors in forward flight, the aeroelastic behavior is mathematically described by means of periodic-coefficient differential equations. Mainly, this is due to the periodicity of the blade relative wind, the cyclic pitch control and the complex rotor-disk inflow distribution generated by the wake vorticity. If these equations are applied for linearized stability analysis around a (periodic) equilibrium condition, aeroelastic dampings may be evaluated exactly through the Floquet theory. However, this theory may be computationally expensive in that requires the evaluation of the so-called fundamental solutions which are as many as the number of state variables describing the rotor blade motion and, in addition, makes the interpretation of the frequencies a difficult task [12], [13]. For this reason, in the past attention has been focused on the application of the multiblade coordinate transformation which consists of expressing the rotating-frame original blade equations in terms of multiblade coordinates in the nonrotating frame [12]. In particular, it has been observed that the constant-coefficient approximation of the aeroelastic equations written in multiblade coordinates in the nonrotating frame yields a satisfactory representation of the rotor aeroelastic behavior, with dampings and frequencies obtained by a standard eigenanalysis (see, for instance, [13]). Moreover, the constant-coefficient aeroelastic representation may be conveniently applied for aeroservoelastic purposes. As a consequence, this approach is widely used for helicopter rotor aeroelastic analysis (especially in the context of multidisciplinary optimization processes and preliminary design).

All this has inspired the procedure for the identification of aerodynamic ROM for rotors in forward flight presented in this paper, which relates multiblade coordinates to corresponding aerodynamic loads in the nonrotating frame. Specifically, observing that in the constant-coefficient representation of linear aeroelastic equations written in multiblade coordinates the relation between multiblade coordinates and corresponding aerodynamic loads in the nonrotating frame may be expressed through frequency-response functions, the procedure consists of the following three steps: (i) using a time marching aerodynamic solver, nonrotating aerodynamic load responses to harmonic multiblade coordinates are evaluated and processed to determine the corresponding frequency response functions; (ii) the matrix collecting all frequency response functions is evaluated for a discrete number of frequencies within an appropriate range, and then its rational matrix approximation is obtained by a least square procedure; (iii) this analytical transfer matrix expression is transformed back into time domain, thus yielding the aerodynamic ROM in terms of a differential form relating multiblade coordinates to the corresponding aerodynamic loads in the nonrotating frame, with inclusion of some additional aerodynamic states (associated to the poles of the rational approximation). Coupling this aerodynamic model with the constant-coefficient rotor blade dynamic equations written in the nonrotating frame in terms of multiblade coordinates gives an aeroelastic state space representation of the type

$$\dot{\mathbf{z}} = \mathbf{A}\,\mathbf{z} \tag{1}$$

where $\mathbf{z}$ is the vector of the multiblade state variables (and additional aerodynamic states), while $\mathbf{A}$ is the constant aeroelastic state matrix. Equation (1) may be conveniently used for the evaluation of aeroelastic dampings and frequencies and, with the introduction of control variables, is suited for aeroservoelastic applications.

For a more detailed description of the identification procedure, the three steps mentioned above are more deeply discussed in the following sections.

Multiblade harmonic responses

The evaluation of the multiblade harmonic perturbation responses is the core of the ROM identification. The accuracy of the final identified ROM depends on the accuracy of the aerodynamic solver applied to predict the harmonic responses. For $q^m(t)$ denoting a degree of freedom of the m-th blade in the rotating frame (blade coordinate), the multiblade coordinates are defined as [12]

$$
\begin{aligned}
q_0(t) &= \frac{1}{N}\sum_{m=1}^{N} q^m(t) \\
q_{nc}(t) &= \frac{2}{N}\sum_{m=1}^{N} q^m(t)\,\cos(n\Omega t) \\
q_{ns}(t) &= \frac{2}{N}\sum_{m=1}^{N} q^m(t)\,\sin(n\Omega t) \\
q_{N/2}(t) &= \frac{1}{N}\sum_{m=1}^{N} q^m(t)(-1)^m
\end{aligned}
$$

where Ω is the rotor angular velocity and N is the number of blades. In addition, q_0 is the collective mode, while the number of cyclic modes, q_{nc}, q_{ns}, depends on the number of harmonics, n, which is $1 \le n \le (N-1)/2$ for N odd, and $1 \le n \le (N-2)/2$ for N even. The coordinate $q_{N/2}$ (differential mode) is present only if N is even. Collecting in the vector $\mathbf{x}^M$ the multiblade coordinates related to all blade degrees of freedom (which, in turn, are collected in the vector $\mathbf{x}^B$), from the equations above it is possible to define a periodic matrix, $\mathbf{T}(t)$, such that

$$\mathbf{x}^B = \mathbf{T}(t)\,\mathbf{x}^M \tag{2}$$

Hence, for a given frequency, ω, and a given (i-th) perturbative harmonic multiblade coordinate

$$x_i^M = M\,\cos(\omega\, t)$$

(with small M), the input to the aerodynamic solver is obtained from Eq. (2). These perturbations are intended about a given periodic reference (equilibrium) motion. Thus, reminding that the final objective is the determination of the constant-coefficient relation between multiblade coordinates and corresponding (multiblade) aerodynamic loads in the nonrotating frame, the aerodynamic loads computed in the blade frame, $\mathbf{f}^B$, are transformed to the nonrotating frame through the relation, $\mathbf{f}^M = \mathbf{T}^{-1}(t)\,\mathbf{f}^B$, and then amplitudes and phases of the ω harmonics of all elements in $\mathbf{f}^M$ (once divided by M) are determined in order to compute the corresponding values of the frequency response functions between x_i^M and the forces $\bar{\mathbf{f}}^M$ (which are the portion of $\mathbf{f}^M$ appearing as forcing term in the constant-coefficient multiblade aeroelastic equations). Specifically, if A_j and ϕ_j are, respectively, amplitude and phase of the ω harmonic of response f_j^M/M, the corresponding transfer function, $E_{ji}(\omega)$, is such that $Re(E_{ji}) = A_j\cos(\phi_j)$ and $Im(E_{ji}) = A_j\sin(\phi_j)$. Note that extracting from the perturbation output only the contribution having the same harmonic of the input implies that, as mentioned above, a constant-coefficient approximation of the relation between multiblade quantities is pursued (in periodic coefficient relations a single-harmonic input yields multi-harmonic outputs), but implies also that only linear(ized) contributions are retained.

Finally, note that if the aerodynamic solver is capable to take into account aerodynamic interaction effects (blade-vortex interaction, for instance) and nonlinearities (wake roll up, for instance), these are not neglected, but rather affect the identified linearized ROM.

Rational matrix approximation

Repeating the multiblade harmonic analysis for all the coordinates in $\mathbf{x}^M$ and for a discrete number of frequencies, the transfer function matrix, $\mathbf{E}(s)$, such that

$$\tilde{\bar{\mathbf{f}}}^M = \mathbf{E}(s)\,\tilde{\mathbf{x}}^M \tag{3}$$

is sampled within an appropriate (from the aeroelastic point of view) frequency range and then, following the approach presented in [14] and [7] its rational matrix approximation is identified. This approach is closely related to the well-known minimum-state technique introduced by Karpel for fixed-wing aerodynamic ROM [11]. Specifically, from the application of a least-square procedure assuring the stability of the identified poles, the transfer function matrix is approximated as

$$\mathbf{E}\,(s) \approx s^2\,\mathbf{A}_2 + s\,\mathbf{A}_1 + \mathbf{A}_0 + \mathbf{H}\,[s\,\mathbf{I} - \mathbf{G}]^{-1}\,\mathbf{R} \tag{4}$$

where $\mathbf{A}_2, \mathbf{A}_1, \mathbf{A}_0, \mathbf{G}, \mathbf{H}$ and $\mathbf{R}$ are real, fully populated matrices. Matrix $\mathbf{G}$ is a square matrix with dimensions related to the number of additional aerodynamic states included in the model due to the delayed effects from wake vorticity [7].

Differential model

Finally, combining Eq. (3) with Eq. (4) and transforming back into time domain yields

$$
\begin{aligned}
\bar{\mathbf{f}}^M(t) &= \mathbf{A}_2\ddot{\mathbf{x}}^M + \mathbf{A}_1\dot{\mathbf{x}}^M + \mathbf{A}_0\mathbf{x}^M + \mathbf{H}\mathbf{r} \\
\dot{\mathbf{r}} &= \mathbf{G}\mathbf{r} + \mathbf{R}\mathbf{x}^M
\end{aligned} \tag{5}
$$

where $\mathbf{r}$ is the vector of the additional aerodynamic states. Coupling Eq. (5) with the constant-coefficient rotor blade dynamic equations written in the nonrotating frame in terms of multiblade coordinates gives the following aeroelastic system

$$
\begin{aligned}
&(\bar{\mathbf{M}} - \mathbf{A}_2)\,\ddot{\mathbf{x}}^M + (\bar{\mathbf{C}} - \mathbf{A}_1)\,\dot{\mathbf{x}}^M + (\bar{\mathbf{K}} - \mathbf{A}_0)\,\mathbf{x}^M = \mathbf{H}\mathbf{r} \\
&\dot{\mathbf{r}} = \mathbf{G}\mathbf{r} + \mathbf{R}\mathbf{x}^M
\end{aligned} \tag{6}
$$

where, for $\mathbf{M}, \mathbf{C}$ and $\mathbf{K}$ respectively representing the periodic structural mass, damping and stiffness matrices in the rotating frame in blade coordinates,

$$\bar{\mathbf{M}} = \overline{\mathbf{T}^{-1}\mathbf{M}\mathbf{T}}; \quad \bar{\mathbf{C}} = \overline{\mathbf{T}^{-1}(2\mathbf{M}\dot{\mathbf{T}} + \mathbf{C}\mathbf{T})}$$

$$\bar{\mathbf{K}} = \overline{\mathbf{T}^{-1}(\mathbf{M}\ddot{\mathbf{T}} + \mathbf{C}\dot{\mathbf{T}} + \mathbf{K}\mathbf{T})}$$

with the overbar denoting mean value (from the expressions above, it is worth noting that the multiblade coordinate transformation operates in the same way as a similarity transformation). Recasting Eq. (6) in state-space format yields Eq. (1).

Numerical results

In this section applications of the aerodynamic ROM for helicopter rotors in forward flight are presented. These concern a four bladed model rotor with hinged flapping and lagging rectangular blades with radius $R = 2$m. The blade chord is $c = 0.121$m, the root-tip twist is $-8°$, and both hinge offsets are equal to 0.25m. It is a soft-in-plane

rotor with the lag spring such that the nonrotating lagging frequency is equal to 0.62/rev, while the nonrotating flapping frequency is equal to 0.1765/rev. For the results presented in the following, the shaft angle has been fixed to $-14°$, the rotor angular speed is $\Omega = 1040$rpm, and momentum trim conditions have been considered. The aerodynamic solver applied for the determination of the transfer functions is based on a Boundary Element Method (BEM) formulation for potential flows [15] that will be briefly described in the following section.

First, the transfer functions identified from the simulations given by the aerodynamic solver and collected in matrix $\mathbf{E}$ are presented and the quality of their rational approximation obtained from Eq. (4) is discussed. Next, the results from the stability analysis of the corresponding finite-state aeroelastic system are shown and compared with those from different aerodynamic modeling. The results presented in this paper deal with a simple rotor model in forward flight conditions such that not strong interactions between rotor wake and blades occur. They have to be considered as preliminary results aimed at demonstrating the feasibility of the aerodynamic ROM approach proposed.

Transfer functions

Now, some of the transfer functions appearing in matrix $\mathbf{E}$ for the problem under examination are shown. As mentioned above, these are determined from harmonic responses predicted by a time marching aerodynamic solver. The aerodynamic solver applied in this work is based on the BEM formulation for potential flows presented in [15]. For φ denoting the velocity potential function (*i.e.,* such that the velocity field is given by $\mathbf{v} = \nabla\varphi$), this BEM formulation stems from the potential-field solution for the arbitrary motion of a lifting body obtained through the following boundary integral representation

$$\begin{aligned} \varphi(\mathbf{x},t) &= \int_{\mathcal{S}_B} \left(\frac{\partial \varphi}{\partial n} G - \varphi \frac{\partial G}{\partial n} \right) \mathrm{d}\mathcal{S}(\mathbf{y}) \\ &- \int_{\mathcal{S}_W} \Delta\varphi(\mathbf{x}_{TE}, t-\tau) \frac{\partial G}{\partial n} \mathrm{d}\mathcal{S}(\mathbf{y}) \end{aligned} \qquad (7)$$

where $\mathcal{S}_B$ denotes the body surface, and $\mathcal{S}_W$ denotes the zero-thickness wake surface where the vorticity generated by the body remains confined. In addition, $G = -1/4\pi\|\mathbf{x}-\mathbf{y}\|$ is the fundamental solution of the Laplace equation, $\partial/\partial n = \mathbf{n}\cdot\nabla$ with $\mathbf{n}$ denotes the outward unit normal to the body surface, whereas $\Delta\varphi(\mathbf{x}_{TE}, t-\tau)$ is the potential discontinuity at the trailing edge location where the wake point was released at the delayed time $t-\tau$. Furthermore, the application of the body surface impermeability condition yields the boundary condition, $\partial\varphi/\partial n = \mathbf{v}_B \cdot \mathbf{n}$, where $\mathbf{v}_B$ denotes the velocity of the body surface points. For $\mathbf{x}$ approaching $\mathcal{S}_B$, Eq. (7) yields an integral equation which may be used to obtain the values of φ on $\mathcal{S}_B$ [15]. Equation (7) is solved numerically by boundary elements, *i.e.,* by the discretization of $\mathcal{S}_B$ and $\mathcal{S}_W$ into quadrilateral panels, assuming φ, $\partial\varphi/\partial n$ and $\Delta\varphi$ to be piecewise constant (zero-th order BEM), and imposing that the equation be satisfied at the center of each body element (collocation method).

Once the potential on the body surface has been determined, the Bernoulli theorem yields the pressure distribution, and hence the aerodynamic forces acting on it may be evaluated. This aerodynamic formulation may

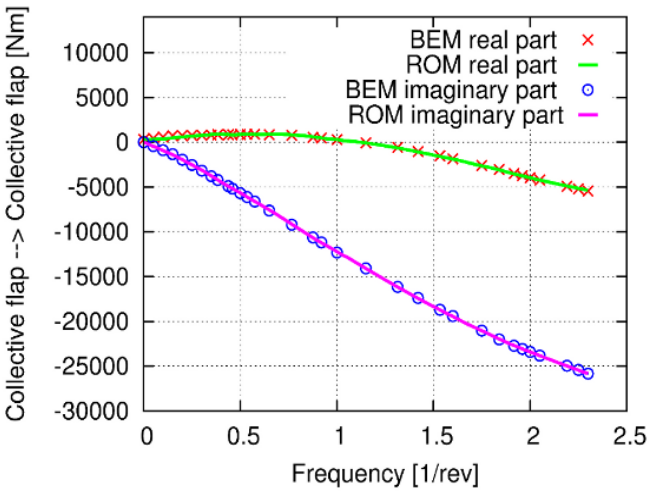

Figure 1. Transfer function between collective flap bending moment and collective flap deflection.

be applied both with prescribed wake shapes and for free-wake analysis. In the free-wake approach, the shape of the wake is obtained as part of the solution. Indeed, once φ on the surface is known, the application of the gradient operator to Eq. (7) yields an integral representation of the velocity field. Thus, at each step of the time-marching procedure, the wake points are moved accordingly to the local velocity field and the shape of the wake is continuously renewed.

Note that in order to determine the transfer functions in the multiblade nonrotating frame, the time-marching solutions to the harmonic inputs have been computed for a large number of rotor revolutions (> 35), and the output Fourier coefficients related to the same harmonic of the input have been evaluated considering a solution time interval free of transient effects, multiple of the period of the harmonic examined, and close to 30 times the period of revolution.

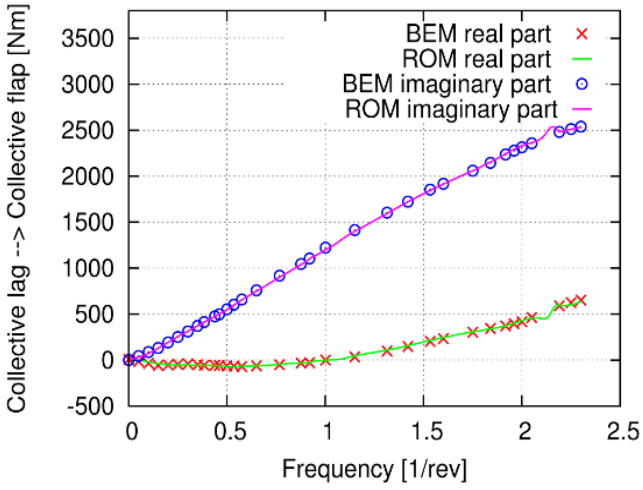

Figure 2. Transfer function between collective flap bending moment and collective lag deflection.

Considering the flight condition corresponding to advance ratio $\mu = 0.16$, Fig. 1 depicts the transfer functions re-

lating the collective flap bending moment to the collective flap deflection, both as derived from the harmonic response predicted by the BEM solver and as approximated through the rational form used in the ROM procedure. Similar comparisons are depicted in Figs. 2-4 which concern, respectively, transfer functions between collective flap bending moment and collective lag deflection, collective lag bending moment and collective lag deflection, and collective flap bending moment and longitudinal cyclic flap deflection. These results show a

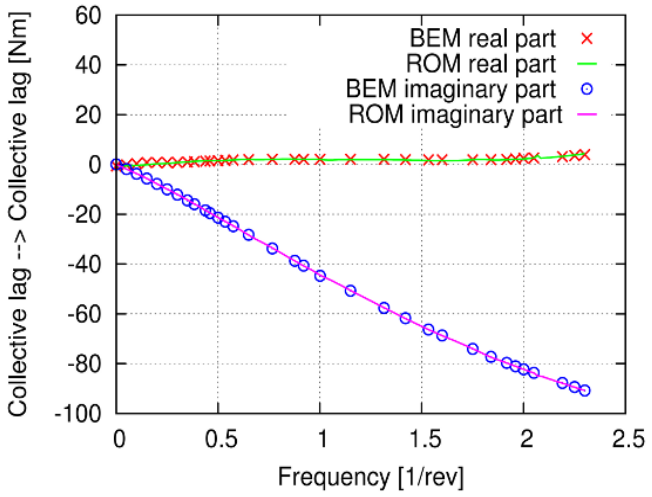

Figure 3. Transfer function between collective lag bending moment and collective lag deflection.

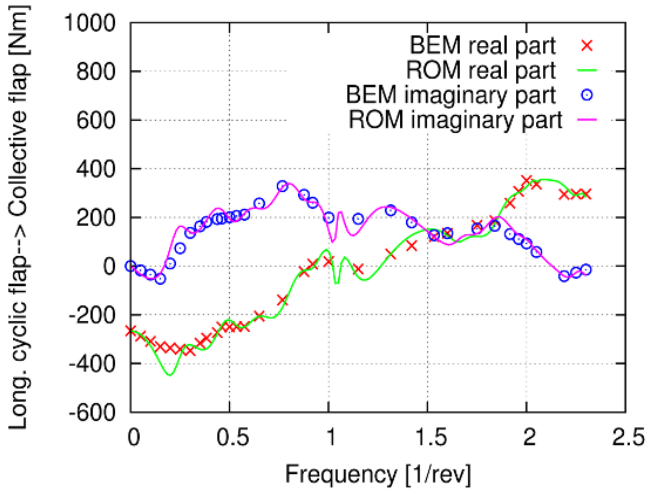

Figure 4. Transfer function between collective flap bending moment and long. cyclic flap deflection.

regular behavior of the transfer functions involving collective modes of both flap and lag degrees of freedom, while a more wavy shape is observed for the transfer function concerning a cyclic mode. This observation remains valid for the rest of the transfer functions not presented here. In addition, Figs. 1-4 demonstrate that the least square approach used in the ROM procedure yields very accurate approximations of the transfer functions, thus assuring also a good level of accuracy of the resulting aerodynamic ROM.

Finally, Fig. 5 shows the accuracy of the aerodynamic ROM proposed. Indeed, for a given 1.2/rev collective-flap input, it compares the longitudinal cyclic flap moment predicted by the time-marching aerodynamic solution with that predicted by the identified reduced-order model in Eq. (5). The higher-frequency small differences between the two solutions are related to constant-coefficient linearization introduced in the process of ROM identification. Anyway, the ROM shows to provide a good approximation of the aerodynamic load arising on the perturbed rotor (worse approximations appear in some coupling differential loads of lower importance for the aeroelastic response prediction).

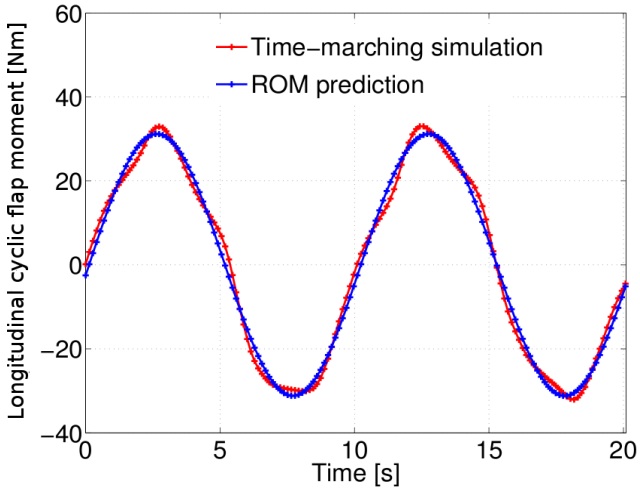

Figure 5. Comparison between time-marching BEM simulation and ROM prediction.

Stability analysis

Next, the aerodynamic ROM identified from the approach proposed has been applied to examine the aeroelastic stability of the model rotor considered.

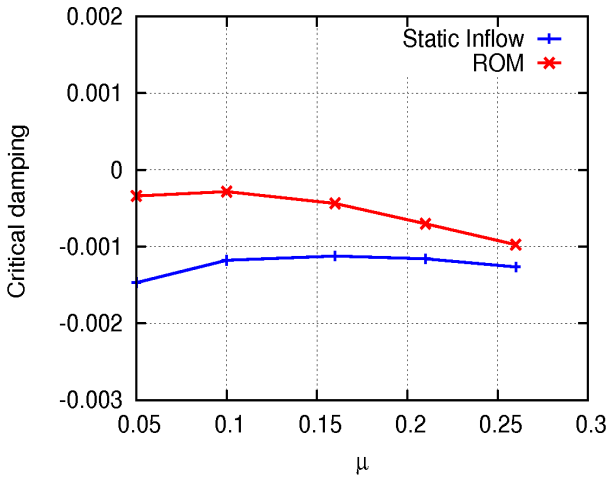

Figure 6. Critical dampings *vs* advance ratio.

Aeroelastic dampings and frequencies have been determined through a standard eigenanalysis of the system in the form of Eq. (1). The critical aeroelastic dampings obtained for advancing ratios $0.05 \leq \mu \leq 0.26$ and zero structural damping are presented in Fig. 6. This figure also shows the comparison with the results obtained replacing the aerodynamic ROM with a model based on a quasi-steady, strip theory approach with Drees static in-

flow. The critical dampings in Fig. 6 are all related to the low-frequency cyclic lag mode (although the other multi-blade lag modes have similar dampings). Those predicted by the ROM solver are very close to the stability margin at low advance ratios, where larger discrepancies between the predictions from the two models occur because of the higher influence of wake effects. As the advance ratio increases the two results tend to be quite similar and this is not surprising in that the rotor configuration is free from strong aerodynamic interaction effects (like blade-vortex interaction, for instance), and this preliminary investigation BEM results have been obtained using a prescribed, undistorted wake shape.

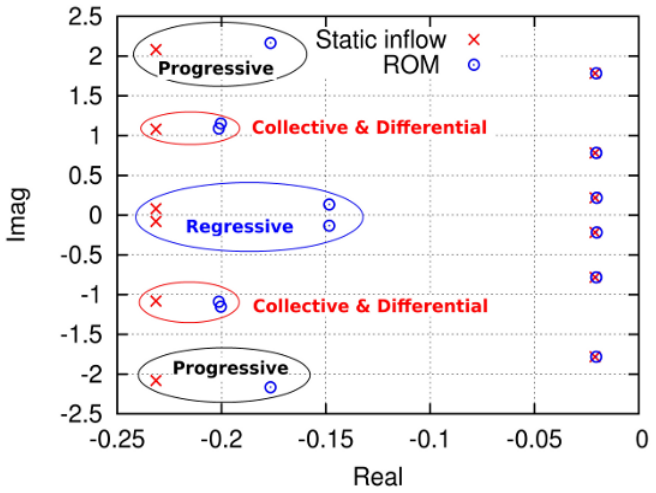

Figure 7. Aeroelastic eigenvalues. $\mu = 0.16$, 1% **structural damping.**

The rotor aeroelastic eigenvalues given by both the proposed aeroelastic ROM and the model based on static inflow for $\mu = 0.16$ and 1% structural damping are depicted in Fig. 7. It shows that the frequencies predicted by the two models are very close, while dampings from static inflow are overestimated, especially those related to the rotor flapping modes (circled ones). Similarly to what occurs when dynamic inflow models are introduced [16], the flap regressing mode is the mode most affected by the application of the aerodynamic ROM.

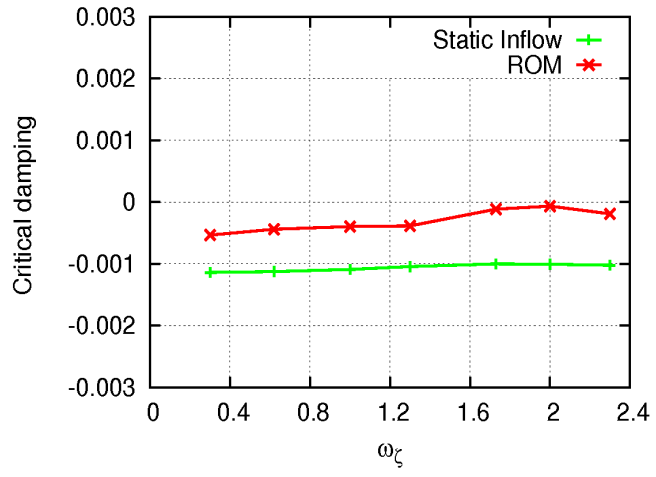

Figure 8. Critical dampings *vs* **lag stiffness.**

Next, the dependence of critical dampings on lag stiffness, ω_ζ, is examined by the aeroelastic ROM based on BEM aerodynamics. Figure 8 shows the critical damping evaluated at $\mu = 0.16$, through aeroelastic ROM and static inflow model, considering soft-in-plane and stiff-in-plane rotor configurations. Akin to what observed in Fig.6, critical dampings are related to the low-frequency cyclic lag mode. Results from the aerodynamic ROM closely approach the stability margin for stiff-in-plane configurations, with the most critical condition occurring for $\omega_\zeta = 2$. A similar trend is shown by the results from static inflow, although higher dampings are predicted and the difference between soft-in-plane and stiff-in-plane configuration results is much smaller.

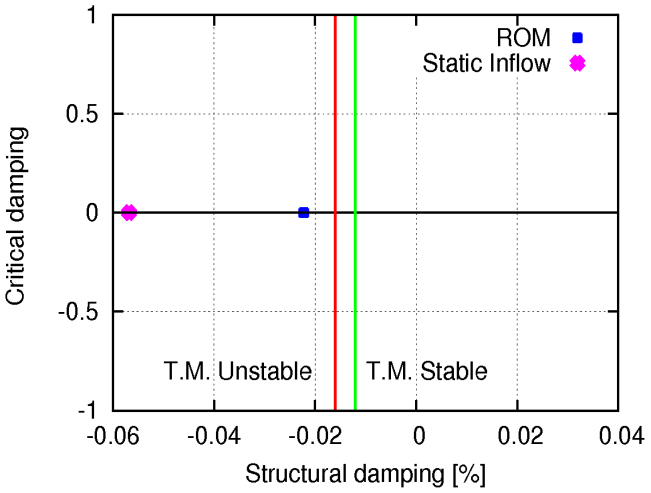

Figure 9. Stability margin comparison.

The main approximations introduced in the proposed process of identification of aerodynamic ROM come from the constant-coefficient assumption in the differential form relating lagrangean variables and loads and from the evaluation of the rational expressions related to the frequency response functions (see sections above).

In order to evaluate the effects of these approximations on the stability analysis, results from ROM are compared with those from the time-marching solution of the aeroelastic system obtained by coupling the blade structural dynamics directly with the BEM aerodynamics solver. Specifically, a fictitious negative lag structural damping is introduced, and the value for which the the stability margin is achieved is determined from the different solvers, at $\mu = 0.16$. Time marching results are obtained with the initial perturbation of the flap collective mode. The stability margins predicted by aerodynamic ROM, static inflow model and time-marching solver are depicted in Fig. 9. The green vertical line corresponds to a negative lag structural damping value, $g = -0.012\%$, for which the time-marching solver presents a stable evolution (Fig. 10), while the structural damping related to red line, $g = -0.016\%$, yields an unstable aeroelastic response (Fig. 11). Thus, the stability margin predicted by the time-marching solver is placed between this two values of g. Figure 9 shows that, at least for the case examined, the effects of the approximations in the ROM approach on the stability analysis are quite small, causing a slight overestimation of the stability margin. A much larger overestimation of the stability margin is given by the static inflow model.

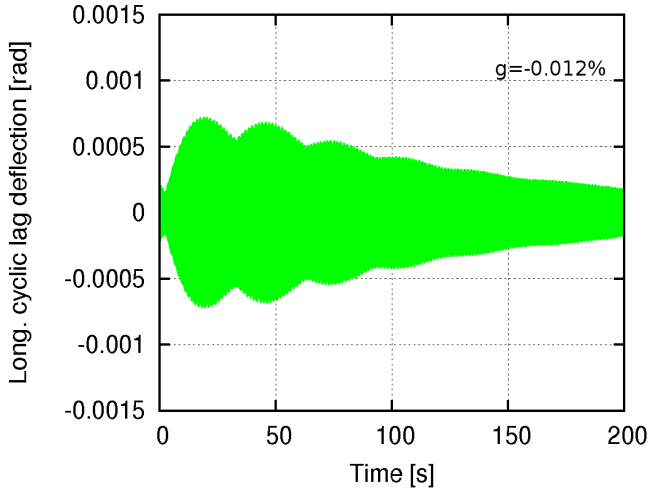

Figure 10. Time-marching stable evolution ($g = -0.012\%$).

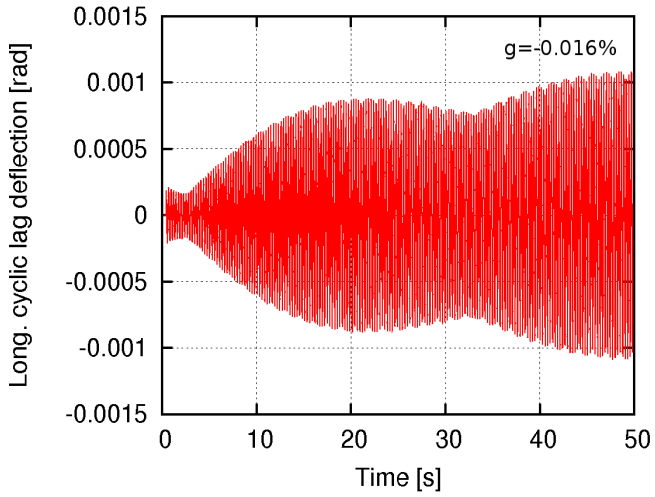

Figure 11. Time-marching unstable evolution ($g = -0.016\%$).

Controlled response

Finally, an aeroservoelastic application of the aerodynamic ROM presented has been accomplished, aimed at the stability augmentation of the zero structural damping configuration, for $\mu = 0.16$. The possibility of control law synthesis based on accurate aeroelastic model, is one of the most important advantages in introducing the aerodynamic ROM.

Specifically, the blade pitch has been assumed as a control variable, $\mathbf{u}$, (actuated by the swashplate, eventually), the ROM concerning the corresponding aerodynamic loads has been identified, and Eq. (1) has been enriched by its contribution thus becoming

$$\dot{\mathbf{z}} = \mathbf{A}\,\mathbf{z} + \mathbf{D}\,\mathbf{u} \tag{8}$$

An optimal control approach has been used to determine the stabilizing constant gain feedback, and its effectiveness on the rotor aeroelastic eigenvalues is depicted in Fig 12. In addition, considering a collective flap rotor velocity perturbation (as that produced by an instantaneous 16m/s vertical gust), Fig. 13 presents the collective lag rotor response evaluated without control (slowly decreasing) compared with that obtained under feedback

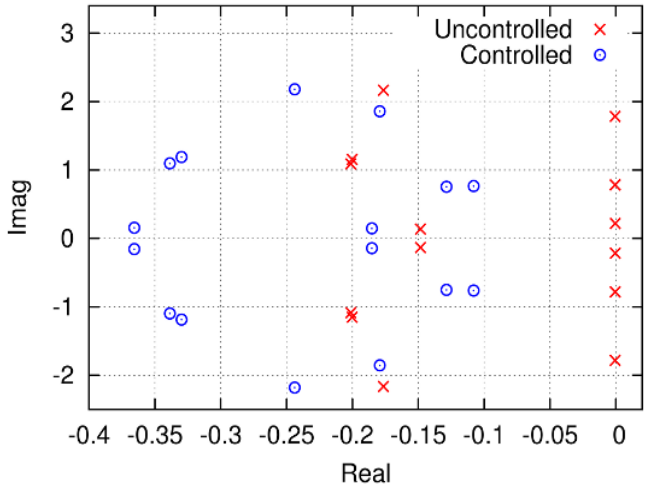

Figure 12. Controlled aeroelastic eigenvalues.

control action. It further demonstrates the efficiency of the control law identified through Eq. (8) in augmenting the stability of the rotor aeroelastic behavior. Because of the nature of the perturbation considered, the corresponding control effort mainly involves collective pitch actuation, with a peak deflection of about 4°. This simple result shows the potentiality of the proposed ROM to be an efficient modeling tool suitable for aeroservoelastic applications.

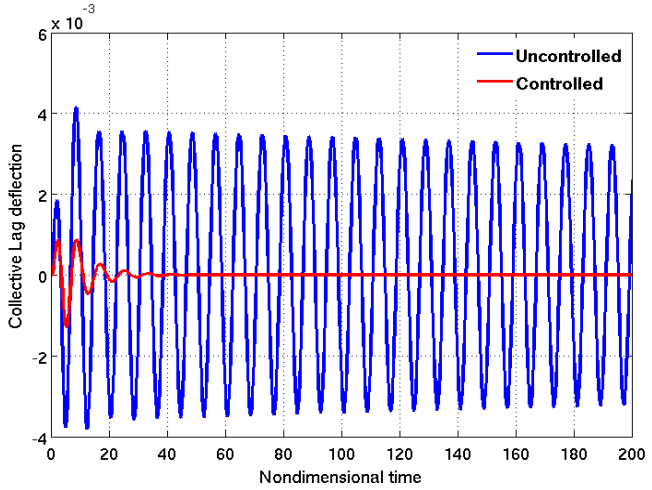

Figure 13. Collective lag response.

Conclusions

An aerodynamic ROM suited for the perturbation aeroelastic analysis of helicopter rotors in forward flight has been presented. Specifically, a procedure for the identification of a linear differential constant-coefficient relation between multiblade coordinates and corresponding aerodynamic loads has been outlined. Thus, the proposed ROM is applicable within aeroelastic systems expressed in terms of multiblade coordinates, under the approximation of constant coefficients (tipically applicable at low- and mid-advance ratio flights of rotors having more than two blades). The identification process is such that (linearized) complex aerodynamic effects (like wake roll up, wake-blade interactions) are included in the ROM if they

are taken into account by the aerodynamic solver used to determine the harmonic responses required by the procedure to evaluate the transfer functions in the multiblade coordinate system. The accuracy of the ROM depends on the quality of the rational approximation of the transfer functions, and the numerical investigation has shown that the proposed least-square approach devoted to this aim is satisfactorily accurate. The aeroelastic stability analysis of a simple rotor model has demonstrated the feasibility of the proposed ROM for the application of the standard eigenanalysis for forward flight conditions, thus avoiding the use of the more costly Floquet theory. In addition, these preliminary results have shown that the stability analysis from simplified theory overestimates the aeroelastic damping (particularly for the flap modes, in the case examined). The comparison between results from the ROM approach and time marching solutions of the aeroelastic system using directly the BEM aerodynamics solver has demonstrated that, for a four-bladed rotor at moderate advance ratio, the approximations introduced in the ROM identification process have a slight influence on the predictions of the aeroelastic behavior. Finally, the applicability of the proposed ROM for aeroservoelastic purposes has been demonstrated. Indeed, using the blade pitch as control variable, a control law for the stability augmentation has been identified and successfully applied starting from the aeroelastic ROM presented.

References

1. Venkatesan, C., Friedmann, P.P, "New Approach to Finite-State Modeling of Unsteady Aerodynamics," *AIAA Journal*, Vol 24, No. 12, 1986, pp. 1889-1897.
2. Gaonkar, G.H., Peters, D.A., "Review of Dynamic Inflow Modeling for Rotorcraft Flight Dynamics," *Vertica*, Vol. 12, No. 3, 1988, pp. 213-242.
3. Peters, D.A., He, C.J., "Finite-State Induced Flow Models, Part II: Three-Dimensional Rotor Disk," *Journal of Aircraft,* Vol. 32, No. 2, 1995, pp. 323-333.
4. Peters, D.A., "How Dynamic Inflow Survives in the Competitive World of Rotorcraft Aerodynamics," *Journal of the American Helicopter Society,* Vol. 54, 2009, pp. 1-15.
5. Zhao, J., "Dynamic Wake Distortion Model for Helicopter Maneuvering Flight," PhD Thesis, School of Aerospace Engineering, Georgia Institute of Technology, 2005.
6. Zhao, J., Prasad, J.V.R., Peters, D.A., "Effect of Rotor Wake Distortion on the Stability of Flapping Dynamics," American Helicopter Society 61th Annual Forum, Grapevine, TX, 2005.
7. Gennaretti, M., Greco, L., "A Time-Dependent Coefficient Reduced-Order Model for Unsteady Aerodynamics of Proprotors," *Journal of Aircraft,* Vol. 42, No. 1, 2005, pp. 138-147.
8. Vepa, R., "On the Use of Padè Approximants to Represent Unsteady Aerodynamic Loads for Arbitrary Small Motions of Wings," AIAA Guidance and Control Conference, New York, AIAA Paper 76-17, 1976.
9. Edwards, J.W., "Application of Laplace Transform Methods to Airfoil Motion and Stability Calculations," 20th Structures, Structural Dynamics, and Materials Conference, St. Louis, MO, AIAA Paper 79-0772, 1979.
10. Roger, K.L., "Airplane Math Modeling Methods for Active Control Design," AGARD-CP 228, 1977.
11. Karpel, M., "Design for the Active Flutter Suppression and Gust Alleviation Using State-Space Aeroelastic Modeling," *Journal of Aircraft*, Vol. 19, 1982, pp. 221-227.
12. Johnson, W., Helicopter Theory, Dover Ed., 1994.
13. Gaonkar, G.H., Peters, D.A., "Use of Multiblade Coordinates for Helicopter Flap-Lag Stability with Dynamic Inflow," *Journal of Aircraft,* Vol. 17, No. 2, 1980, pp. 112-118.
14. Morino, L., Mastroddi, F., De Troia, R., Ghiringhelli, G.L., Mantegazza, P., "Matrix Fraction Approach for Finite-State Aerodynamic Modeling," *AIAA Journal*, Vol. 33, No. 4, 1995, pp. 703-711.
15. Morino, L., Gennaretti, M., "Boundary Integral Equation Methods for Aerodynamics," Computational Nonlinear Mechanics in Aerospace Engineering, edited by S. N. Atluri, Vol. 146, Progress in Aeronautics and Astronautics, AIAA, Washington, D.C., 1992, pp. 279-320.
16. Peters, D.A., Gaonkar, G.H., "Theoretical Flap-Lag Damping With Various Dynamic Inflow Models," *Journal of the American Helicopter Society,* Vol. 25, 1980, pp. 29-36.